VOL. 23, NO. 3, 2024, 67-72
elektrika.utm.my
ISSN 0128-4428

ELEKTRIKA
Journal of Electrical Engineering

Comparison between Two Different Fractal Koch Position for Reflecting Intelligent Surface (RISs)

Nur Syahirah Binti Mohd Yaziz[1], **Mohamad Kamal Bin A. Rahim**[1], **Noor Asmawati Binti Samsuri**[1] and **Farid Bin Zubir**[2]

[1]Advanced RF and Microwave Research Group (ARFMRG), Faculty of Electrical Engineering, Universiti Teknologi Malaysia, 81310 UTM Skudai, Johor, Malaysia.
[2]Wireless Communication Center (WCC), Faculty of Electrical Engineering, Universiti Teknologi Malaysia, 81310 UTM Skudai, Johor, Malaysia.

*Corresponding author: syahirah92@graduate.utm.my, mdkamal@utm.my, asmawati@utm.my, faridzubir@utm.my

Abstract: The paper focuses on investigating the fractal shape placement of metasurface reflectors at the X-band frequency for Reflecting Intelligent Surface (RIS). The proposed reflector adopts a square shape, with the fractal intersection on a Rogers RO5880 substrate measuring 0.51 mm in thickness. The graph illustrating the S-parameter and reflection phase exhibits the simulated outcomes for various fractal positions. Furthermore, the bandwidth of the proposed reflector was determined by analyzing the simulation results. The impact of the incident wave angle on the proposed reflector was observed to shift along the horizontal axis. Mainly, the reflector with the inward fractal shape position demonstrated better performance and a wider bandwidth compared to the outward fractal substrate.

Keywords: metamaterial reflector, fractal shape position, intelligent surface

Article History: received 28 June 2024; accepted 3 November 2024; published 30 December 2024

1. INTRODUCTION

Future generations of wireless communication networks will be able to create smart radio environments due to a new wireless transmission technology called Reconfigurable Intelligent Surfaces (RISs). RIS function as reflectors and enable the individual modification and optimization of the phase response on adjustable unit element metasurfaces for beam-steering, focusing, and other relevant applications. In [1], the two main RIS categories that are utilized in wireless networks are examined. The initial category will be integrated into structures, such as walls, and will be controlled by wireless network operators through a software controller to adjust radio waves for purposes like improving network coverage. RISs of the second type will be integrated into items like smart shirts equipped with health-tracking sensors [2], communicating data to mobile phones using radio waves reflected by cell towers.

The study of regular metasurfaces and reconfigurable metasurfaces' key research advancements is examined in detail, with an emphasis on the modulation of amplitude, phase, polarization, and multi-dimensional forms as described in [3]. Metasurface [4] is primarily used to control the amplitude of incident electromagnetic waves, allowing for reflection, absorption, or transmission. The phase response properties of the metasurface, on the other hand, depend on the size, shape, rotation mode, and substrate material type of the metasurface unit. Asymmetric metasurface elements can induce phase variances in electromagnetic waves that are transmitted or reflected in the perpendicular direction [5]-[8]. Nevertheless, the metasurfaces mentioned earlier are limited to controlling just one aspect, like amplitude [9], phase [10], or polarization of incoming electromagnetic waves [11]. In-depth examination of amplitude, phase, polarization, and multi-dimensional modulation functionalities, described in [12], uncovers significant advancements in traditional metasurfaces and newly developed reconfigurable metasurfaces. The metasurface is typically utilized to control the amplitude of incident electromagnetic waves by reflecting, absorbing, or transmitting their energy. However, the metasurface [13] unit's phase response characteristics are significantly affected by its size, shape, rotation mode, and substrate material type. A non-symmetrical metasurface unit allows for achieving the phase disparity of electromagnetic waves transmitted or reflected in a perpendicular direction. Only one of the metasurfaces mentioned can manipulate the amplitude, phase, or polarization of incoming electromagnetic waves.

Based on [14], the square shape structure had been known to meet the essential reflecting characteristics such as simple structure, high angular stability, polarization-independent and small operation band, which offer the good performance of the reflecting structure. Due to the concern of the bandwidth frequency coverage in the reflecting area, most design produce a narrow bandwidth coverage. This paper presents the fractal Koch structures: outward and inward, that are studied in terms of the

performance of the reflecting characteristics. The structures are analysed in order to have a better understanding and comparison between these structures.

In this paper, the study regarding the position of the fractal Koch position structures shown in terms of the resonance frequency f_r, bandwidth (BW), incident wave angle effect and current distribution effect. The metamaterial reflector designs for the two fractal Koch position structures: outward fractal shape and inward fractal shape, had been explained in details Section 2. The analysis and discussion of the results for all two designs in terms of f_r, BW, incident wave angle effect and current distribution effect are presented in Section 3. The conclusion of the study is presented in Section 4.

2. FRACTAL KOCH UNIT CELL DESIGN

A fractal does not need to be an exact replica to be considered a shape. The primary criteria for being classified as a Fractal is having inherent and repeating similarities within their shapes. Fractals were first described by Benoit Mandelbort in 1975 as a way to categorize structures that are challenging to define using Euclidean geometry [15]. Koch curve have been widely used to minimize the schemes and maintain the wideband frequency coverage [16].

The patch element's electrical length (L) must be approximately half the free-space wavelength, calculated using equations (1) and (2), involving ε_{eff}, ε_r, and c, for resonance frequency, f_r to occur. This study introduces a metamaterial reflector design based on fractal geometry featuring outward and inward angles.

$$f_r = \frac{c}{2L\sqrt{\varepsilon_{eff}}} \tag{1}$$

$$\varepsilon_{eff} = \sqrt{\frac{\varepsilon_r + 1}{2}} \tag{2}$$

The Koch curve is achieved by repeating a specific construction an infinite number of times, which demonstrates that it is the limiting curve. To prove that this construction produces a genuine curve as its limit, consider Figure 1 displays the process of creating the iteration. The ln is separated into three equal parts, each one being one-third of the original length. Then, the ln scale is rotated by 60° and -60° in the second part and undergoes further scaling to one-third and a translation in the last part. Equation (3) can be used to determine the value of the hypotenuse h. Figure 2 illustrates the fractal location featuring both outward and inward components.

$$h = \sqrt{\left(\frac{l_n}{2}\right)^2 + \left(sin\left(\frac{\pi}{3}\right)\left(\frac{l_n}{3}\right)^2\right)} \tag{3}$$

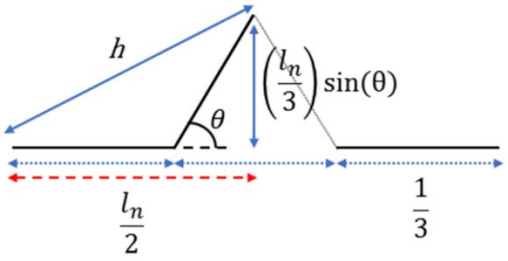

Figure 1. Segments that form the basic of the Koch fractal

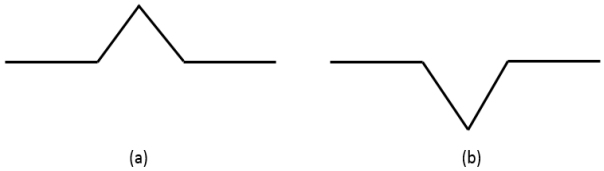

Figure 2. Illustration of fractal: (a) outward fractal shape (OFS) and (b) inward fractal shape (IFS)

Figure 3 depicts the unit cell geometry of the suggested metamaterial reflector. The Rogers RT5880 substrate, with a thickness of 0.51 mm, a dielectric constant of 2.2, and a loss tangent of 0.0009, features outward and inward fractal iteration patterns on its surface. To reflect most of the incident power, a full ground copper plane layer is utilized.

The CST Microwave Studio software was utilized to design and simulate the unit cell. The dimensions of the unit cell are as follows: length and width both equal to 11.43 mm, while a and b are both 7.4 mm, and the height is 0.51 mm. The copper film is represented as a metallic layer with an electrical conductivity of σ=5.8×107 S/m. The frequency domain solver was performed using a unit cell boundary condition in the *xy* direction and Floquet ports in the z-direction to obtain S-parameters. Table 1 tabulate the dimensions of the outward and inward fractal shape.

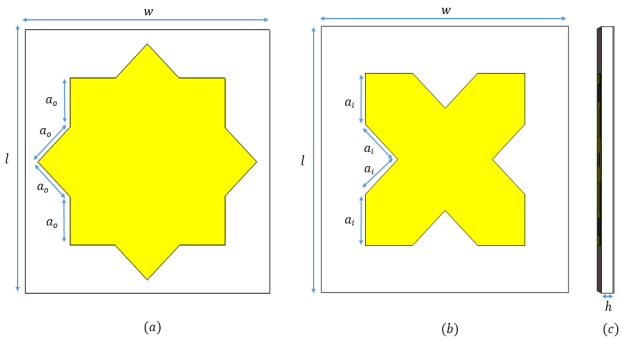

Figure 3. The metamaterial reflector structure: (a) front view outward fractal shape (OFS), (b) front view inward fractal shape (IFS) and (c) side view

Table 1. The parameter of the unit cell design

Parameters (mm)	Fractal shape position	
	Outward	Inward
Width of substrate (w)	11.43	11.43
Length of substrate (l)	11.43	11.43
Substrate thickness (h)	0.51	0.51
Length of fractal	(a_o) 7.53	(a_i) 7.40

3. SIMULATION RESULTS

The advanced EM simulator CST software is used to perform the simulation with a frequency solver. The simulation gathers the S-parameter outcomes. Figure 4 displays the simulated reflection and absorption magnitudes. In relation to the law of energy conversion, the sum of reflection, absorption and transmission must be equal to one, represented as R(w)+A(w)+T(w)=1. The transmission is nonexistent as a result of the solid copper metal layer on the back of the proposed reflector. The reflectance of the metamaterial reflector with outward and inward fractal for a normal incident wave is 0.90 and 0.93, respectively. The reflection stage repeats every 360° with a bandwidth of -90° to +90°. The outward fractal metamaterial reflector has a bandwidth of 0.29 GHz, covering from 11.90 GHz to 12.19 GHz, whereas the inward fractal metamaterial reflector has a bandwidth of 0.37 GHz, covering from 11.86 GHz to 12.23 GHz as listed in Table 2.

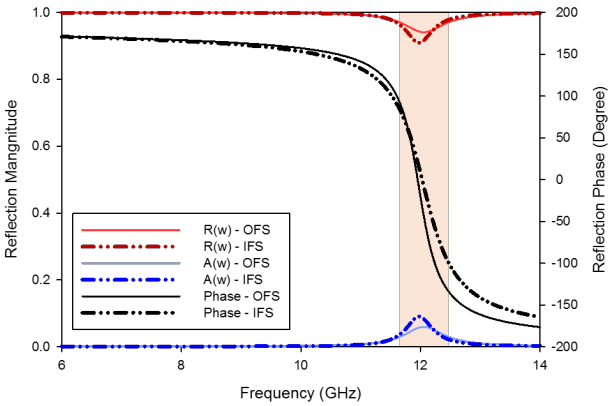

Figure 4. Reflection, absorption magnitude and reflection phase of the proposed metamaterial reflector

Table 2. Bandwidth comparison between these two fractal shapes

Fractal shape position	Bandwidth (GHz)
Outward	0.29
Inward	0.37

3.1 The incident wave angle effect

Any IRS design must have structures capable of maintaining their reflecting characteristic of incident electromagnetic waves. For normal incident angles, metamaterial reflectors normally may reflect EM waves very high because they can induce the magnetic resonance in a lossy substrate and attenuate. However, when the incidence angle varies to a bigger excitation angle, the reflectance will generally decrease because the ability of the metamaterial structures to induce the magnetic resonance in the substrate is reduced. Figure 5 shows the illustration of the variation of the incident waves angle.

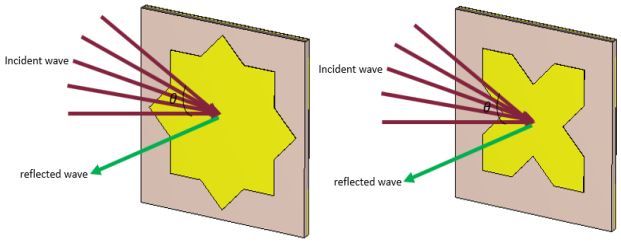

Figure 5. Illustration of the incident waves angle

Figure 6 shows the simulated result of the reflection values for moving the incident wave angle from 0^0 to 80^0. The reflection value at 12 GHz frequency decreased from 0.90 to 0.5 with a slightly shift in frequency to a higher frequency. These phenomena happen because the incident wave is not properly going through the proposed reflector and it affect the percentage of reflected power to drop. The reflection phase is shown in Figure 7 whereas the incident angle is bigger, the bandwidth become narrow.

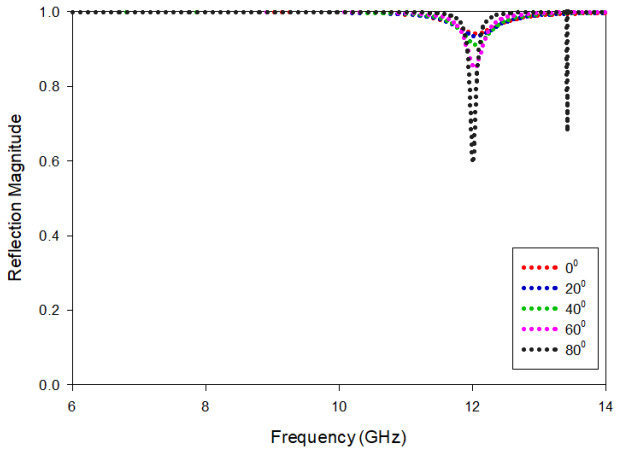

Figure 6. Reflection magnitude of the outward fractal metamaterial reflector

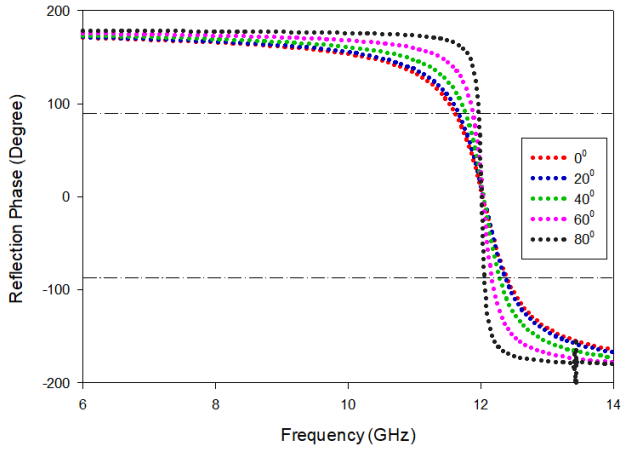

Figure 7. Reflection phase of the outward fractal metamaterial reflector

Inward fractal metamaterial reflector is depicted in Figure 8, showcasing the simulated transverse electric wave (TE) mode at various excitation angles (0°, 20°, 40°, 60°, and 80°). At 12 GHz, the reflectance value for the 0° excitation angle is 0.92. As the incidence angle changes to 20°, the reflectance decreases slightly to 0.90. When the incidence angle is adjusted to 40°, the reflectance at 12 GHz reaches a resonant response of 0.87. As the incidence angle continues to increase to 60°, the reflectance drops to 0.8. Lastly, at 80°, the reflectance decreases to 0.5, demonstrating that the maximum angle that allows for at least 80% reflection of incident electromagnetic waves is 60°. Beyond this angle, the structure cannot maintain its reflective properties. In summary, Figure 8 demonstrates the simulated TE mode for the inward fractal metamaterial reflector at various excitation angles, while Figure 9 shows the corresponding reflection phase, indicating a smaller bandwidth as the incidence angle increases.

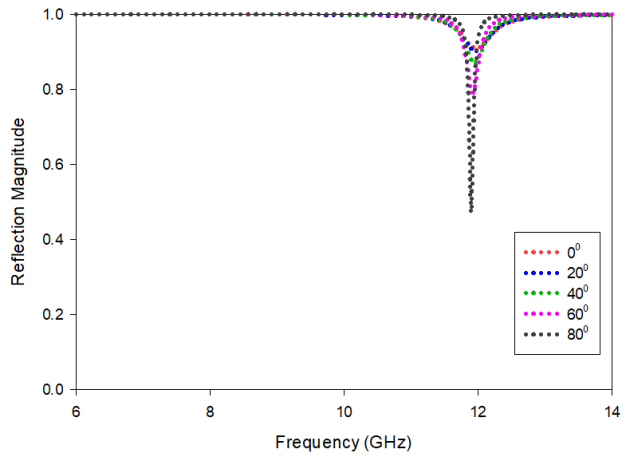

Figure 8. Reflection magnitude of the inward fractal metamaterial reflector

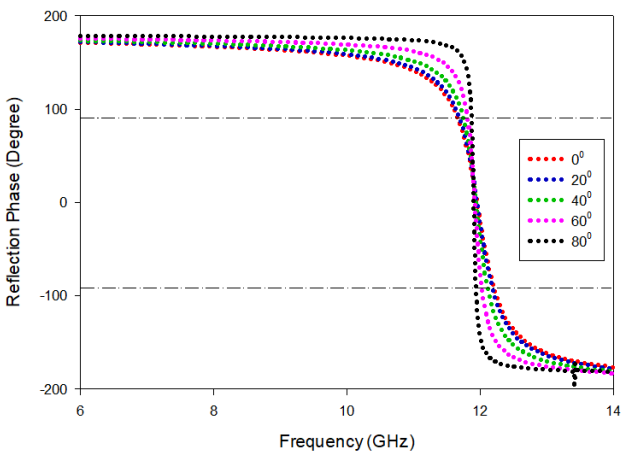

Figure 9. Reflection phase of the inward fractal metamaterial reflector

The operating bandwidth of the proposed outward and inward fractal reflector using RO5880 substrate can be seen clearly in Table 3. The outward bandwidth value will be narrowed if the incident wave is moving from 0° to 80°. For the inward fractal reflector, as the incident angle increases from 0^0 to 80^0, the bandwidth will be decreases from 0.37 GHz to 0.15 GHz. From here it clearly be seen that the inward fractal shape position gives better bandwidth performance compared to the outward fractal shape position.

Table 3. Bandwidth of the outward and inward fractal at 12GHz at different incident wave

Fractal shape position	**Bandwidth (GHz)**				
	0^0	**20^0**	**40^0**	**60^0**	**80^0**
Outward	0.29	0.27	0.25	0.2	0.09
Inward	0.37	0.35	0.31	0.27	0.15

3.2 The current distribution effect

A simulation is conducted to analyze the current distribution at the resonance frequency. The simulated surface currents for the E-field and H-field are displayed in Figure 10. Based on Figure 10 (a) and Figure 10 (c), it is evident that the power loss concentration is greater on the +y and -y axes of the structure than other areas, aligning with the electric component of the incident EM waves. Likewise, as shown in Figure 10 (b) and Figure 10 (d), surface current concentration is greater at the +x and -x axis of the structure, and is at its lowest at the -y and +y axis because of the magnetic aspect of EM waves aligning with the x-axis of the structure. The present distribution displays identical behavior to the E-field scenario.

Figure 11 shows the power loss distribution for both design of outward and inward fractal. As seen in Figure 11 (a) and (b) the outward fractal tends to produce higher mutual coupling between edges of neighboring patches compared to Figure 11 (c) and (d). In other words, the mutual coupling effect can reduce the gain of the reflector.

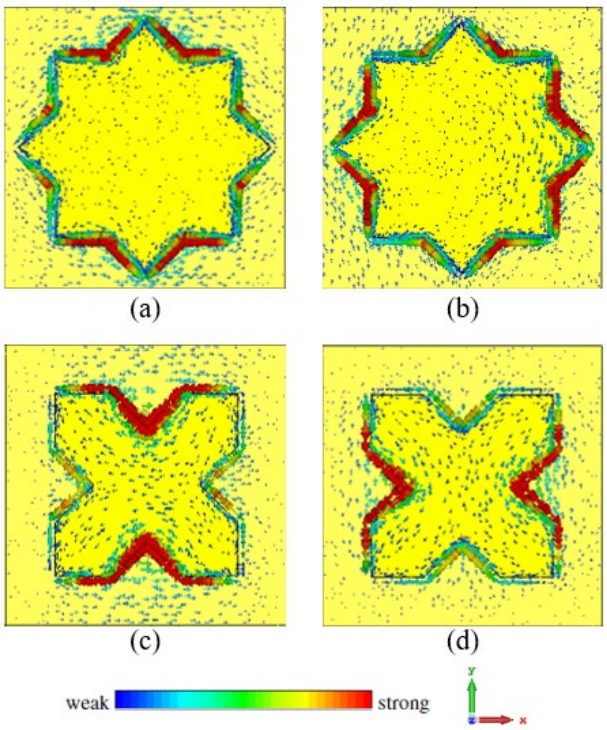

Figure 10. Surface current for (a) outward fractal E-field, (b) outward fractal H- field, (c) inward fractal E-filed and (d) inward fractal H-field

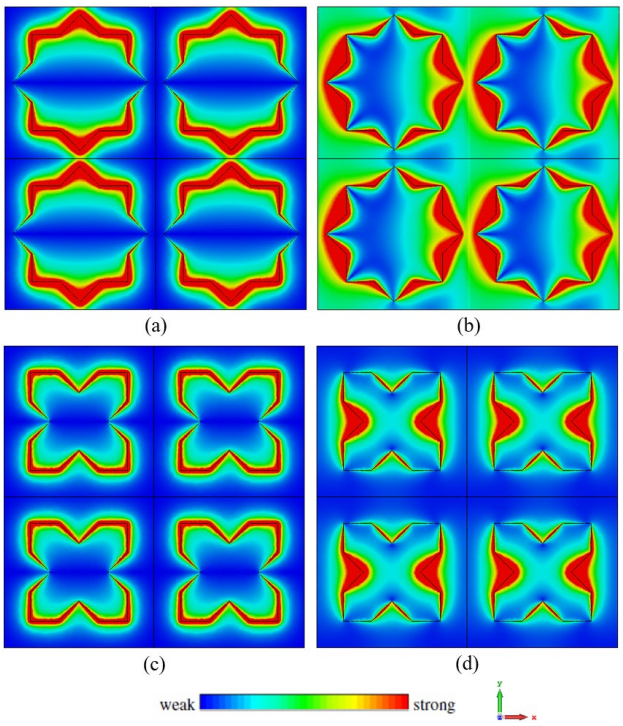

Figure 11. Power loss distribution for (a) outward fractal E-field, (b) outward fractal H- field, (c) inward fractal E-filed and (d) inward fractal H-field

4. CONCLUSION

As conclusion, the reflector proposed in this study has been designed and simulated using CST software with various fractal shapes on substrate RO5880 to obtain the overall simulated results. The inward fractal gives an improvement of 8% of bandwidth enhancement compared to the outward fractal shape. Besides, in term of current distribution, the inward fractal shape produces less mutual coupling to the neighborhood shape compared to the outward fractal shape.

ACKNOWLEDGMENT

The authors thank the Ministry of Higher Education (MOHE) for supporting the research work, Research Management Center (RMC), Universiti Teknologi Malaysia (UTM), Faculty of Electrical Engineering for the support of the research under grant no.04M34, 5F591 (FRGS/1/2023/TK07/UTM/02/15).

REFERENCES

[1] S. Atapattu, R. Fan, P. Dharmawansa, G. Wang, J. Evans, and T. A. Tsiftsis, “Reconfigurable Intelligent Surface Assisted Two-Way Communications: Performance Analysis and Optimization,” IEEE Trans. Commun., vol. 68, no. 10, pp. 6552–6567, 2020.

[2] A. Kobyakov and A. R. Zakharian, “Estimate of Throughput Improvement Due to a Metasurface Reflector in 5G Millimeter-Wave Links,” IEEE Antennas Wirel. Propag. Lett., vol. 22, no. 3, pp. 636–640, 2023.

[3] M. Di Renzo et al., "Smart Radio Environments Empowered by Reconfigurable Intelligent Surfaces: How It Works, State of Research, and The Road Ahead," in IEEE Journal on Selected Areas in Communications, vol. 38, no. 11, pp. 2450-2525, Nov. 2020.

[4] Zahra S, Ma L, Wang W, Li J, Chen D, Liu Y, Zhou Y, Li N, Huang Y and Wen G, Electromagnetic Metasurfaces and Reconfigurable Metasurfaces: A Review. Front. Phys.2021.

[5] M. K. Emara, D. Kundu, K. MacDonell, L. M. Rufailand S. Gupta, “Coupled Resonator-Based Metasurface Reflector with Enhanced Magnitude and Phase Coverage”. TechRxiv, 14-Apr-2023.

[6] J. Li, S. Xu, J. Liu, Y. Cao, and W. Gao, “Reconfigurable Intelligent Surface Enhanced Secure Aerial-Ground Communication,” IEEE Trans. Commun., vol. 69, no. 9, pp. 6185–6197, 2021.

[7] J. C. B. Garcia, A. Sibille, and M. Kamoun, “Reconfigurable Intelligent Surfaces: Bridging the Gap between Scattering and Reflection,” IEEE J. Sel. Areas Commun., vol. 38, no. 11, pp. 2538–2547, 2020.

[8] Q. Guo and F. Hao, “Comments on ‘Wideband Microwave Absorber Comprising Metallic Split-Ring Resonators Surrounded with E-Shaped Fractal Metamaterial,’” IEEE Access, vol. 9, pp. 121302–121304, 2021.

[9] F. Costa and M. Borgese, “Electromagnetic Model of Reflective Intelligent Surfaces,” IEEE Open J. Commun. Soc., vol. 2, no. June, pp. 1577–1589, 2021.

[10] M. I. Khan, Z. Khalid, S. A. K. Tanoli, F. A. Tahir, and B. Hu, “Multiband linear and circular polarization converting anisotropic metasurface for wide incidence angles,” J. Phys. D. Appl. Phys., vol. 53, no. 9, 2020.

[11] Y. Han, X. Li, W. Tang, S. Jin, Q. Cheng, and T. J. Cui, "Dual-Polarized RIS-Assisted Mobile Communications," IEEE Trans. Wirel. Commun., vol. 21, no. 1, pp. 591–606, 2022.
[12] J. B. Gros, V. Popov, M. A. Odit, V. Lenets, and G. Lerosey, "A Reconfigurable Intelligent Surface at mmWave Based on a Binary Phase Tunable Metasurface," IEEE Open J. Commun. Soc., vol. 2, no. April, pp. 1055–1064, 2021.
[13] X. HOU, X. LI, X. WANG, L. CHEN, and S. SUYAMA, "Some Observations and Thoughts about Reconfigurable Intelligent Surface Application for 5G Evolution and 6G," ZTE Commun., vol. 20, no. 1, pp. 14–20, 2022.
[14] Yaziz, N. & Rahim, MKA & Zubir, Farid & Samsuri, Noor Asmawati. (2023). A Comparison of the Bandwidth Coverage for Different Metasurface Reflector Shapes. 1423-1424. 10.1109/USNC-URSI52151.2023.10237802.
[15] R. DuHamel and F. Ore, "Logarithmically Periodic Antenna Designs," IRE Int. Conv. Rec., vol. 6, 1958.
[16] M. N. A. Karim, M. K. A. Rahim, and T. Masri, "Fractal Koch Dipole Antenna for UHF Band Application," *Microw. Opt. Technol. Lett.*, vol. 51, pp. 2612–2614, 2009.